Using FTIR to determine toxic gases in fires with Li-ion batteries

Abstract

Batteries, in particular Li-ion batteries, are seen as an alternative to fossil fuels in the automotive sector. Li-ion batteries, however, have some safety issues including possible emissions of toxic fluorine containing compounds during fire and other abuse situations. This paper demonstrates the possibilities to use the Fourier Transfer Infrared Technique (FTIR) to assess some of the most important compounds, including HF and the far less often measured POF_3 and PF_5. The study is conducted in the Cone Calorimeter with different solvents used in Li-ion batteries. The measurements show that, in addition to HF, with a known high toxicity, POF_3 is emitted and can be quantified using FTIR.

Petra Andersson[a,*], Per Blomqvist[a], Anders Lorén[a], Fredrik Larsson[a,b]
[a]SP Technical Research Institute of Sweden, Box 857, SE-501 15 Borås, Sweden
[b]Department of Applied Physics, Chalmers University of Technology, SE-412 96 Göteborg, Sweden

*Corresponding author: petra.andersson@sp.se

Keywords: FTIR, Li-ion batteries, Fire emissions, electrolyte, HF, POF_3, $LiPF_6$

Introduction

Batteries are used in more and more applications and are seen as an important alternative to fossil fuels as energy carrier in the automotive sector. Several types of batteries are used today and more are being developed. One of the most common types of batteries today is lithium-ion (Li-ion) batteries due to their high energy and power densities. Li-ion batteries have, however, some safety drawbacks with their organic based flammable electrolyte. Compared to many other battery technologies, Li-ion batteries also have a smaller stable operation region of temperature and voltage. Outside this region, Li-ion batteries can undergo a thermal runaway resulting in gassing and fire, and potentially explosion [1, 2]. Thermal runaway can occur if a Li-ion cell is exposed to increased temperatures. The occurrence of a thermal runaway is determined by the rate of cell internal heat generation and the rate of the cooling (heat transfer from cell to adjacent materials). The cell chemistry, i.e. electrode materials and electrolyte composition (including additives) can play a dominant role in the thermal runaway onset temperature. However, typically thermal runway onset values found in literature are temperatures of 120-150 °C [3]. Other types of abusive conditions, e.g. overcharge or deformation can also result in venting of gasses and thermal runaway reactions.

A Li-ion battery cell consists of anode and cathode electrodes, a separator between them in order to avoid direct electrical contact between them, and electrolyte to allow for transport of Li-ions between the electrodes during charge/discharge. The anode typically consists of graphite on an aluminium current collector while the cathode typically consists of metal oxides (e.g. $LiCoO_2$, $LiN_xM_yC_zO_2$) on a copper current collector. The electrolyte and the binder (e.g PVdF) in the active electrode materials contain fluorine in some form. Additional fluorine can be present in additives, e.g. fluorine content in flame retardants in the electrolyte. The electrolyte of a Li-ion cell consists of organic solvents (e.g. ethylene carbonate (EC), diethyl carbonate (DEC), dimethyl carbonate (DMC)), a lithium salt and a number of

additives. The far most used Li-salt today is hexafluorophosphate ($LiPF_6$) due to its attractive performance despite its moderate thermal stability and fluorine content.
Under abusive conditions, fluorine containing compounds might be emitted. Compounds that can be emitted and pose a danger include the chemical species in the oxidation and thermal breakdown of the initial $LiPF_6$ salt solution. This breakdown can take different routes, a simplified route is described here.

When heated in a dry and inert environment $LiPF_6$ decomposes to lithiumfluoride (LiF) as solid and phosphorouspentafluoride (PF_5) as gas [4, 5, 6, 7]

$$LiPF_6 \rightarrow LiF + PF_5 \quad (1)$$

In contact with moisture/water PF_5 reacts to form phosphorous oxyfluoride (POF_3) and hydrogen fluoride HF [7] (Other routes are also possible as discussed by Lux et.al. [6])

$$PF_5 + H_2O \rightarrow POF_3 + 2HF \quad (2)$$

$LiPF_6$ is highly susceptible to hydrolysis by even trace amounts of moisture [8]. When heated in moisture/water $LiPF_6$ can directly form LiF, POF_3 and HF [7].

$$LiPF_6 + H_2O \rightarrow LiF + POF_3 + 2HF \quad (3)$$

PF_5 also reacts with HF to form hexa-fluoro-phosphoric acid (HPF_6) [9]:

$$PF_5 + HF \rightarrow HPF_6 \quad (4)$$

Phosphorous oxyfluoride (POF_3) can react to form several fluorinated phosphoric acids, mono-fluoro-phosphoric acid (H_2PO_3F), di-fluor-phosphoric acid (HPO_2F_2) hexa-fluor-phosphoric acid (HPF_6), and phosphoric acid (H_3PO_4) [10]. The fluorinated phosphoric acids can react with water and yield HF and form phosphoric acid as a final product [10]:

$$H_3PO_4 \underset{H_2O}{\overset{HF}{\rightleftharpoons}} H_2PO_3F \underset{H_2O}{\overset{HF}{\rightleftharpoons}} HPO_2F_2 \underset{H_2O}{\overset{HF}{\rightleftharpoons}} HPF_6 \quad (5)$$

In addition to PF_5, POF_3 and HF, fluorinated phosphoric acids [10] can be formed and ultimately give HF and phosphoric acid (H_3PO_4) when completely reacted with water. Overheating in a Li-ion battery cell can also result in formation of toxic fluoro-organic compounds [11] and organic esters [6].

The toxicity of these gases is not fully established. The Swedish Work Environment Authority has exposure limits for total fluorides, HF and phosphoric acid but lacks data for the remaining substances [12]. The NGV[i] for total fluorides are 2 mg/m^3 and HF has a TGV[ii] of 2 ppm. NIOSH (National Institute for Occupational Safety and Health, USA) states that HF has a IDLH (Immediately Dangerous to Life and Health) value of 30 ppm. No exposure limits are given for PF_5 and POF_3, however, their chlorine analogues, PCl_5 and $POCl_3$, have NGV values of 0.1 ppm. The toxicity might, however, differ between the chlorine and fluorine species and there is no general rule like “fluorine is always more toxic”. But, still, the limits

[i] ”Nivågränsvärde” Mean value threshold in a working environment
[ii] ”Takgränsvärde” Maximum allowed concentration in a working environment

are low and gases evolved from battery fires are certainly of great concern to both the fire fighters, people close to a Li-ion battery in e.g. electric vehicles or in the close vicinity of the fire. Other gases emitted from electrolytes, especially under non-fire conditions include e.g. H_2, CO, CH_4, C_2H_6 [13, 14, 15], this paper focuses however on the fluorinated species and in particular on HF, PF_5 and POF_3 due to their toxicity and potential toxicity. Means to measure these substances in fire situations are sought for in order to be able to compare different Li-ion battery cells and fire situations including extinguishment.

There is only limited information available on PF_5 and POF_3 measurement methods. Possible measurement techniques were searched for in the literature and it was soon concluded that a possible solution was to use the Fourier Transform Infra-Red (FTIR) technique as all three gases have absorbance in the infrared spectra while no information was found on e.g. suitable florescence wavelength for these species. This study focused on FTIR methodology since it has the advantage of detection of several substances simultaneously without interfering with the chemical equilibria in the gas phase. Wet chemical methodologies followed by chromatography and suitable detection were ruled out due to uncertain kinetics and equilibria.

Studies have been performed on decomposition rate [16, 17] and degradation mechanisms [18] of the electrolyte but only few studies are available on PF_5 and POF_3 emissions. Yang, Zhuang and Ross [5] report measurements of these gases conducted using TGA (Thermal Gravimetry Analysis) and FTIR on pure $LiPF_6$ salt and salt solved in EC, DMC, PC (propylene carbonate), and EMC (ethyl methyl carbonate). Eshetu et al. [19] studied the different solvents used in the electrolytes without the salt with a focus on Heat Release Rate (HRR) from the different solvents and also toxicity of the combustion gases from the solvents. However as no $LiPF_6$-salt was included in these tests the toxicity was similar to most organic solvents. In a more recent study by Eshetu et al. [20] also fluorinated species such as HF and POF_3 were evaluated for different electrolytes using the Tewarson apparatus and the FTIR technique. Ribiere et al. [21] have also performed a study on pouch cells in the Fire Propagation or Tewarson apparatus where FTIR was used to measure toxic gases including HF but other fluorinated gases were not evaluated.

This paper presents work on developing a method suitable to be used in fire experiments. The method was used in the cone calorimeter where HRR [22] was measured together with gases emitted including HF, POF_3 and PF_5 in order to investigate possible influence of the burning conditions, fuel composition and water addition on the amounts of HF, POF_3 and PF_5 produced. The measurements were conducted using the FTIR technique and a first step in the study was to demonstrate the suitability of the FTIR technique for measurements of these substances in fire situations. To this end the FTIR equipment was first calibrated for HF, POF_3 and PF_5. Then, tests were conducted on pure salt and $LiPF_6$ solutions in different electrolyte solvents at various concentrations. The solvents included in this study were Dimethyl carbonate (DMC) and Dimethoxyethane (DME) and Propylene carbonate (PC). The solutions were introduced to a propane flame as a spray at different flow rates or onto a metal plate in the flame in order to achieve different burning conditions and fuel composition.

FTIR instrumentation and calibration

The measurement system used consisted of an FTIR spectrometer, a gas cell, sampling lines, filters for removing particulates before the gas cell and a pump that continuously drew sample gas through the cell. The system is specified in Table 1.

The FTIR used had a calibration for a number of components when delivered from factory. These components included e.g. CO_2, CO and HF. It was seen that the factory calibration for HF was not sufficiently accurate for the intended use of the instrument and the instrument was recalibrated to include more spectral information and a wider concentration range i.e. include the full spectral band of HF and a concentration range from 18 ppm to 1245 ppm. The calibration of HF was made using a dynamic dilution system where a water solution of known HF-concentration was injected with a calibrated syringe pump (*BRAUN Perfusor Compact S*) into a heated stream of nitrogen in a T-junction configuration. The nitrogen flow was pre-heated (180 °C) using a 7 m long heated PTFE tubing. The T-junction was constructed from a cylindrical block of aluminium, 100 mm long and 40 mm diameter. A 10 mm diameter ~80 mm long mixing chamber had been drilled into the centre of the block and the inner surfaces of the chamber was coated with PTFE. The heated nitrogen flow was directed through the length of mixing chamber (connections for 6 mm tubing at both ends of the chamber) and the liquid flow was applied with a 1.0 mm inner diameter PTFE tubing inserted into the middle of the mixing chamber perpendicularly to the nitrogen flow. The T-junction and all connections were enclosed in a heating box which maintained a temperature of 200 °C. The flow rate of the water solution was low in comparison with the gas flow. For e.g. 177 ppm HF concentration a flow rate of 1 mL/h was used for a 1.0 M HF solution in a nitrogen flow of 2 nL/min. This resulted in a water concentration of about 1 %-by volume in the nitrogen stream. The nitrogen stream was heated to 180 °C.

The quantification limit (LOQ) for HF with the recalibrated FTIR was determined to 2 ppm. In addition was the FTIR calibrated for PF_5 and POF_3. Calibration gas mixtures were prepared for this purpose by dilution of PF_5 (99%, ABCR) and POF_3 (99%, ABCR) in nitrogen atmosphere using gasbags (Flexfoil, SKC). Sample bags were flushed with dry nitrogen to remove adsorbed water from the walls prior to dilution of the analytes. For PF_5 this was step was especially important and approximately 100 bag volumes had to be replaced before acceptably stable PF_5 mixtures could be prepared.

Tests were conducted to record the spectral bands of POF_3 as a basis for calibration of the FTIR. An important part of the calibration work was further to investigate the thermal stability of POF_3. The spectral range of interest of POF_3 (116 ppm) is shown in Figure 1; several distinctive absorption bands can be seen.

Figure 1 Spectral bands of POF_3.

Three spectral bands are shown centred around the wavenumbers 871 cm^{-1} (P-F symmetrical stretch), 991 cm^{-1} (P-F asymmetrical stretch) and 1416 cm^{-1} (P-O stretch). The two latter vibrations are the strongest. The spectral information of POF_3 is summarized in Table 2.

A quantitative calibration was made for POF_3 using flushed gas bags where known volumes of POF_3 gas were injected into a known volume of nitrogen gas. The concentrations produced for the calibration were: 25 ppm, 100 ppm, 200 ppm, 300 ppm and 416 ppm. Spectral regions around 871 cm^{-1} and 1416 cm^{-1} were used for a CLS (classical least squares) calibration and

water was included as an interfering component. The calibration was linear and a regression yielded a 0.98 R^2 fit. The quantification limit (LOQ) for POF_3 was calculated to 6 ppm.

The thermal stability of POF_3 at both room temperature and at an elevated temperature was investigated in order to check that the calibration mixtures prepared in gas bags were stable in varying temperature and to see if any significant decomposition would take place in the heated sampling and measurement system. The investigation showed that POF_3 is very stable at room temperature in a gas bag diluted with N_2, which makes it possible to prepare quantitative calibration standards. No special effort in drying the bags was conducted in this case. Figure 2 shows the spectra of ~200 ppm POF_3 from two different gas bags, stored for 8 and 33 minutes respectively at room temperature before measurement. No decomposition at room temperature could be detected from this test. The half-life for POF_3 in N_2 at 170 °C[iii] was about 15 minutes according to the measurements shown in Figure 3, which means that there is no significant self-decomposition taking place in the measurement system during the ~10 s response time of the FTIR measurement set-up.

Figure 2 Spectra of ~200 ppm POF_3 measured from two separate Flexfoil bags at 8 min and 33 min after preparation.

Figure 3 Series of spectra of 41 ppm POF_3 kept at 170°C in the FTIR gas cell for different times (0, 8 and 31 minutes).

To prepare PF_5 standard gas blends for calibration it was found that the gas bags used needed to be dried by flushing with N_2 in order to remove any remaining water. Otherwise no significant spectral bands apart from those of POF_3 and HF could be seen. This is because the PF_5 added to the bag was hydrolysed even by the small amounts of water that was present in the bag, to form the decomposition products POF_3 and HF. The bags were subsequently thoroughly dried before adding PF_5.

By using flushed bags it was possible to locate the spectral bands of PF_5 [5]. The spectral range of interest for PF_5 of nominally 200 ppm PF_5 in N_2 is presented in Figure 4 (1027, 1017, 956 and 946 cm^{-1}). As seen in Figure 4 bands from POF_3 (1416, 991 and 871 cm^{-1}) are also seen despite careful flushing of the bag. PF_5 has two stretching modes according to Yang et al. [5]. These are most probably the bands at 1017 cm^{-1} and 946 cm^{-1}. The remaining two bands found, 1027 cm^{-1} and 956 cm^{-1}, must thus originate from unidentified decomposition products of PF_5. The bands are listed in Table 3.

Figure 4 Spectral bands of PF_5 and decomposition products from 200 ppm PF_5 in N_2. Decomposition occurred although the Flexfoil bag was flushed with dry N2 prior to standard preparation.

[iii] The investigation of decomposition at an elevated temperature was made with a cell temperature of 170 °C which was slightly lower compared to the standard cell temperature of 180 °C.

Heating tests with the Cone Calorimeter

The first step in our study was to investigate whether the same type of decomposition products as Yang et al. [5] found, could be found in tests where the salt and its solutions in electrolyte were heated in an open container with radiative heating in a Cone calorimeter [22]. Further, combustion tests were conducted where the vapour was ignited to investigate how combustion would change the type of decomposition products.

The sample was placed in a small (~40 mm diameter) metal bowl which was placed under the cone shaped heating element of the Cone calorimeter. The irradiation of the sample was in the range of 10-15 kW/m^2. The FTIR was connected to the exhaust duct of the Cone calorimeter 52 cm away from the extended centre of the radiating cone. Separate tests were conducted with only solvent (DME and PC), the pure $LiPF_6$ salt, the saturated solution of $LiPF_6$ salt and the solvent, one test of each. The sample size in these tests was limited, in the order of 5 g salt. This is a rather small sample in the cone calorimeter in relation to the dilution of the exhausts. Still the spectral bands could be easily observed.

Figure 5 shows the spectral bands of POF_3 in the test where pure $LiPF_6$ salt was thermally decomposed in the cone calorimeter. HF was also identified in this experiment. There are no traces of PF_5 or any additional decomposition products apart from POF_3 in the spectral range shown in Figure 5.

Figure 5 Spectral bands of decomposition products from pure Lithium hexafluoride ($LiPF_6$) in an evaporation test with the Cone calorimeter.

A spectrum from an evaporation experiment with a saturated solution of $LiPF_6$ salt in PC is shown in Figure 6. Overlaid in this figure is a spectrum from an evaporation tests with pure PC. The spectral band from the solvent is shown around 1100 cm^{-1} together with the three bands of POF_3 at 871 cm^{-1}, 991 cm^{-1} and 1416 cm^{-1} demonstrating the clear identification of the different substances in the evaporation experiment.

Figure 6 Spectrum from evaporation test with $LiPF_6$ mixed in Propylene carbonate (PC) with overlaid spectrum from evaporation of pure PC.

Similarly Figure 7 shows a spectrum from an evaporation test with a saturated solution of $LiPF_6$ salt in DME together with an overlaid spectrum from an evaporation experiment with pure DME. Also here the spectral band from the solvent is seen around 1100 cm^{-1} together with the three bands of POF_3 at 871 cm^{-1}, 991 cm^{-1} and 1416 cm^{-1}.

Figure 7 Spectrum from evaporation test with $LiPF_6$ mixed in Dimethoxyethane (DME) solid line overlaid by spectrum of DME only (dotted line).

A Test wase also conducted where the saturated solution of $LiPF_6$ salt in DME, was ignited by the electric spark igniter in the Cone calorimeter. In thise tests the same level of external radiative heat flow was used as for the evaporation tests discussed above (10-15 kW/m^2). A series of spectra (overlaid) are shown in Figure 8 from the test with $LiPF_6$ salt in DME. One can clearly see the characteristic spectral features of POF_3 during the period of combustion (2-95 s). Also HF was seen in the spectrum during this period (not shown in Figure 9). The spectral band from the solvent is shown only in the first spectrum and in the spectrum from 67 s. The combustion efficiency must have decreased at this time but extinction was not recorded until 95 s. Figure 9 shows the spectrum from 54 s with a spectrum of DME from the evaporation test overlaid. Interesting is the two additional peaks, one at 1027 cm^{-1} and one at 1034 cm^{-1}, which do not originate from POF_3 and most probably not from DME. The peak at 1027 cm^{-1} was also found in the calibration tests with PF_5 where PF_5 was partly decomposed (see Figure 4).

Figure 8 Series of spectra from fire test with $LiPF_6$ mixed in Dimethoxyethane (DME). Spectra measured at 5 s, 42 s, 54 s and 67 s after start of heat exposure. Ignition at 2 s after start. Flame-out at 95 s.

Figure 9 Spectrum from the fire test with $LiPF_6$ mixed in DME at 54 s from start of test. Overlaid by spectrum from evaporation test with DME (solid line).

Figure 10 shows a series of spectra (overlaid) from the test with $LiPF_6$ salt in PC. The spectral bands of POF_3 (the band at 991 cm^{-1} can be clearly seen in the figure) were seen in the spectra during the period of combustion (71-170 s). Also HF was seen as in the spectra during this period (not shown). The spectral band from the solvent is clearly shown in the spectra before ignition.

Figure 10 Series of spectra from fire test with $LiPF_6$ mixed in Propylene carbonate (PC). Spectra measured at 53 s (solid line, before combustion), 103 s (during combustion), 116 s (during combustion) and 162 s (during combustion) after start of heat exposure. Ignition at 71 s after start. Flame-out at 170 s.

Figure 11 Spectrum from the fire test with $LiPF_6$ mixed in PC at 128 s from start of test (dotted line). Overlaid by spectrum from evaporation test with PC (solid line).

Figure 11 shows the spectrum collected at 128 s into the combustion test with $LiPF_6$ salt in PC. A spectrum of pure PC has been overlaid. Also here one can see the two additional peaks which do not originate from POF_3, one at 1027 cm^{-1} and one at 1034 cm^{-1}.

The combustion tests with electrolyte solvents of $LiPF_6$ salt showed that HF and also POF_3 are present in the combustion effluents, while PF_5 is not present. Further, unidentified spectral absorption bands indicate the presence of an additional, possibly fluorine containing,

decomposition product. The identification of the origin of the unidentified absorption peaks would be important to fully understand the decomposition of $LiPF_6$. The presence of POF_3 is an important finding as this emission can be important to be included in a toxicity evaluation of the fire effluents.

Burner tests with electrolyte

An experimental set-up, with a simple diffusion propane burner with the possibility to introduce solvent/salt solutions and water into the flame through needles, was designed in order to be able to vary the salt/solvent concentration and combustion conditions in the test flames. This was done in order to investigate possible effects on toxic gas production from varying combustion conditions and from water used as extinguishing media.

The needle solution was chosen in order to produce a spray into the propane flame to make sure that the total amount of solvent/salt introduced was combusted. The propane burner was a very simple one, about 2 cm in diameter and holes were drilled in the side about 0.5 cm below the rim to introduce the needles, a schematic illustration of the set-up is provided in Figure 12.

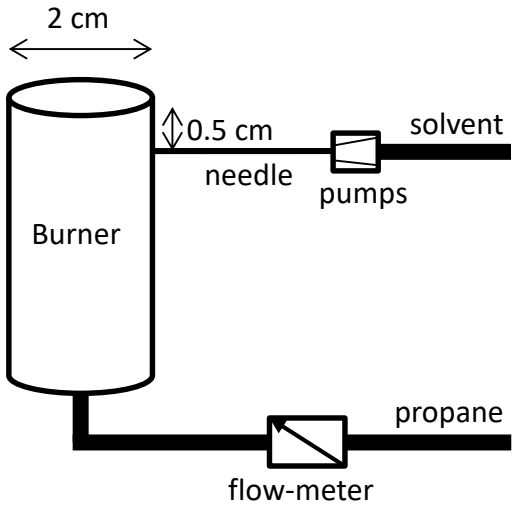

Figure 12. Schematic illustration of burner

The amount of propane introduced was controlled by a variable area flow-meter. The amount of electrolyte inserted was controlled by two HPLC pumps. In the cases where salt was included, the solutions had been prepared before introduction into the HPLC pumps. Solutions of $LiPF_6$ (99 %, Sigma-Aldrich) were prepared by dilution in dimethylcarbonate (DMC, 99% Sigma-Aldrich) and 1,2-dimethoxy ethane (DME, 99% Sigma-Aldrich). The DMC solutions were 1.0 M and 0.4 M respectively and the DME solution was 0.4 M.

The HRR from the combustion was measured by using Oxygen Consumption Calorimetry on the effluents quantitatively collected in the Cone calorimeter hood. FTIR measurements were made in all tests. Tests were conducted with different propane/solvent ratio. Also the way the solvent and salt were introduced into the flame was varied (either through the needle into the flame or onto a metal plate in the flame) and the amount of salt was varied.

Some tests were conducted where water was introduced into the flame. The duration of these tests was however, limited. Despite careful design of needles that were custom made for this study, problems were encountered with creating a stable spray for long periods of time.

An example of test results using the spray into the flame is presented in Figure 13 and Figure 14 where 18 ml/min with 0.4 M salt solved in DME was introduced in the flame as a spray during 2.5 minutes. A full set of test results is available in Andersson et al. [23]. In Figure 13 the HRR is presented on the left hand axis together with the HF concentration in the exhaust duct on the right hand axis. The HRR curve includes the HRR from the propane flame also; the timing for the introduction of the electrolyte spray is clearly seen as the HRR increases sharply. In Figure 14 from the same test, HF concentration in the smoke duct is presented on the left hand side and the POF_3 concentration in the duct on the right hand side axis.

When studying the graphs it is important to remember that the concentrations are measured in the exhaust duct. These depend on the gas flow in the exhaust duct and the amount of salt and electrolyte introduced into the flame. They should not be considered as the concentration in the vicinity of a burning Li-ion battery in an electrified vehicle but are only presented here as concentrations in order to evaluate changes in amount produced due to changes in flame composition etc.

Figure 13. HRR and HF concentration in a test where 18 ml/min with 0.4 M salt solved in DME was introduced in the flame during 2.5 minutes.

Figure 14 HF and POF_3 concentration as a function of time in a test where 18 ml/min with 0.4 M salt solved in DME was introduced in the flame during 2.5 minutes.

Similar curves for a test where 18 ml/min of 1 M salt in DMC was introduced into the flame as a spray during two minutes are shown in Figure 15 and Figure 16. As seen the results are similar to the case with 0.4 M salt in DME as presented in Figure 13 and Figure 14, i.e. the spray introduction is clearly seen as a sharp increase in the HRR and the HF and POF_3 concentration increases with a slight delay. A difference is however seen in the HF/POF_3 ratio.

Figure 15 HRR and HF concentration during a test where 18 ml/min of 1 M salt solved in DMC was injected as a spray during two minutes.

Figure 16 HF and POF_3 concentration as a function of time for a test where 18 ml/min of 1 M salt solved in DMC was injected as a spray during two minutes.

The tests using the spray introduced into the burner all showed that the HRR was increased immediately upon injection of the electrolyte while the increase in the HF and POF_3 concentration increased was somewhat delayed. This is caused by the 12 s integrating time of the FTIR analysis equipment and could also be due to delays in the filter and sampling system and to some extent to the delays in the pump system for introducing the salt and solvent.

An example of a result from a test where DMC and salt was introduced into the flame in a much slower pace, i.e. 1.8 ml/min during 5 minutes is given in Figure 17. In this case the electrolyte flow had to be inserted onto a metal plate in the flame as it was not possible to get a spray at this low rate. As only a small amount of electrolyte was introduced into the flame no change in HRR could be observed. Still both HF and POF_3 were detected. The time delay here is significant; this is due to the long transportation time through the pump system with this small pump flow. Also the delay in HF detection due to delay in the sampling system is more pronounced here as the amount of HF produced is much lower due to the lower rate of electrolyte introduction.

Figure 17. HF and POF_3 measurements from a test where 1.8 ml/min of 1M salt solved in DMC was introduced onto a metal plate in the flame

The tests conducted are summarized in Table 4 together with the HF/POF_3 ratio as calculated from the FTIR measurements in the cone calorimeter. As seen in the table the FTIR measurements showed that both HF and POF_3 were always present in the combustion effluents when electrolytes were burning. The measured concentration of HF was always significantly higher than the measured POF_3 concentration.

Despite careful design of needles it was difficult to obtain a stable spray. The needles were clogged in many cases and tests had to be interrupted. In some cases the measured HRR was lower than anticipated indicating that the flow through the pump was lower than anticipated or that incomplete combustion of the electrolyte occurred due to that some electrolyte was released as a beam rather than a spray. Table 4 gives some insights into the uncertainties involved in these measurements e.g. by studying Tests B and C which repeats the same conditions and results in a HF/POF_3 ratio of 14 and 20 respectively. A similar variation is seen between Tests E and G with a HF/POF_3 ratio of 23 and 12 respectively.

Studying Test B, E and G one sees that Tests E and G with a larger propane/electrolyte ratio resulted in a HF/PO3 ratio of 23 and 12 respectively while the ratio was 14 for Test B, i.e. varying the propane/electrolyte ratio does not affect the HF/POF_3 ratio.

Tests E and G's range of 12-23 covers to some extent the results from Tests H and I where water was sprayed into the flame for some period during the test which resulted in a HF/POF_3 ratio of 8 and 16 respectively. The results from Test H are shown in Figure 18 where water was sprayed into the propane/electrolyte flame at time 3 minutes until 3:45. As seen it seems that the water injection causes the POF_3 content to increase. The same ratio is also kept initially when the electrolyte injection was stopped and water was let trough the pump and needle in order to clean the needle from time 5 minutes until 7 minutes. However, as shown in

Figure 19, no such effect was observed in Test I and thus it is not possible to make any conclusions concerning the water influence on the fluorinated species generated even if the HF/POF_3 ratio seems to be on the lower side of the ratio measured in the case without water. The reason for the limited effect of the water spray can be that the water sprayed into the flame was limited compared to the amount of water already present due to the combustion of the propane and electrolyte (water vapour from the FTIR measurement is presented as a dotted line in Figure 18 and Figure 19).

Figure 18 HF and POF_3 concentration for the electrolyte injection during time 2 minutes until 3 minutes 40 and water cleaning of the system during time 5 minutes until 7 minutes. Water was sprayed into the propane/electrolyte flame from time 3 minutes until 3 minutes 40.

Figure 19 HF and POF_3 concentration for the electrolyte injection during time 9 minutes until 10 minutes 30s. Water was sprayed from time 9 minutes 50 until 10 minutes 30.

A notable difference is however seen between Test A and the other tests. In Test A, 0.4 M DME was used while DMC was used in all other tests. The HF/POF_3 ratio is 53 in Test A while it differs between 8 and 23 for the other tests. This ratio is especially interesting in the light of Test F where the HF/POF_3 ratio is 20 for a 0.4 M DMC solution. Eshetu et al. [19] indicates that the toxicity of the combustion gases depends on the solvents used when studying unburned hydrocarbons, aldehydes and soot in oxygen lean conditions, i.e. linear carbonate esters result in less toxic gases than cyclic carbonates. Both DMC and DME are linear which gives no guidance in this matter. In addition Eshetu et al. [19] studied only the solvents without any salt, and did not study fluorinated compounds. DME and DMC differ significantly in heat of combustion. DME has a Heat of combustion of almost 28 kJ/g compared to about 14.6 kJ/g for DMC. Also the solubility of the salt differs significantly between DME and DMC.

All tests showed that the POF_3 appeared a bit earlier than HF; this was especially apparent in Test D where the electrolyte/salt solution was introduced onto a metal plate at a low flow rate in the flame. It is known that loss of HF occurs in the measurement system and especially in the sampling filter [24]. The effect is most significant at measurements of low concentrations as the proportion captured in the filter in such cases is high compared to the total amount HF sampled through the filter. An effect of HF-losses in the filter is an initial increased response time (until the sampling system is saturated) that can be significant especially in measurements of low concentrations. Selected filters used in the measurements were analysed for total fluorine content. The analysis results showed that the amounts lost in the filter were low, normally around 5 % on weight basis.

In situations of low smoke gas temperatures in a cone calorimeter test there are other possible sources of losses of HF. Water could potentially condense on the wall surfaces of the smoke gas duct and also in the sampling probe. In all tests the propane burner was used for a couple of minutes before introducing the electrolyte which increased the temperature in the duct above 100°C before electrolyte with salt was introduced in most cases but not above 170°C. However, these effects have not been investigated further in the work presented here.

Conclusions

This work shows that it is possible to use FTIR to measure HF and POF_3 in real time in Li-ion electrolyte experiments with and without combustion in the Cone calorimeter, equipment that is commonly used in fire testing. The detection limit for the FTIR used was determined to 2 ppm for HF and 6 ppm for POF_3. No other gases were sought for except PF5. No attempt was made to further understand the decomposition of the $LiPF_6$ salt in the electrolyte.

The possibility to use in fire testing apparatuses is important in order to be able to evaluate emissions from batteries in real scale and in its final application, and not only in apparatuses used for investigating the chemistry such as TGA. Fire behaviour of Li-ion battery cells has recently been progressed by Larsson et al. [25] in their study on Li-ion cells in the Single Burning Item (SBI) apparatus including measurements of HRR and gas emissions [26] and by Fu et al. [27] using the Cone calorimeter to study fire performance of 18650 cells. Another analytical technique that has been reported lately is FTIR+MS by Gachot et al.[28] in their study on non-fluorinated gaseous emissions from swelling Li-ion cells.

The FTIR method presented here was used on electrolytes combusted in a propane flame in the Cone calorimeter. Both HF and POF_3 were detected in all experiments. It is an important finding that POF_3 is emitted together with HF from combustion. This can increase the toxicity of the fire effluents. The amount of POF_3 is significant with a HF/POF_3 ratio between 8 and 53, i.e. between 1.9 % and 12.5 % POF_3 compared to HF. Eshetu et.al. [20] recently reported a value of 2.75% in the fire propagation apparatus. The toxicity of POF_3 is not known and more information is needed to fully understand the importance of POF_3 in toxic evaluation of Li-ion cells especially as POF_3 can be emitted under other cell venting situations.

PF_5 could not be detected in any of the tests. The reason for this is most probably the high reactivity of this species. This was demonstrated by the difficulty to produce a calibration gas mixture for PF_5.

Given the uncertainties involved in the tests it was not possible to determine the effect of combustion parameters (such as solvent/propane ratio, concentration of salt or the way the salt/solvent was introduced into the flame) on the gases produced.

A possible difference was seen in HF/POF_3 ratio depending on solvent used. The solvent might have an impact on the amount of substances emitted in a fire situation. Eshetu et al. [19] suggested an evaluation scheme for different solvents considering combustion behaviour and other properties such as viscosity. Considering the combustion parameters, DME would be a poor choice. This evaluation scheme does, however, not include fluorinated compound toxicity. Given the toxicity of HF and possible also POF_3, a replacement for the $LiPF_6$ salt is important to improve the safety for Li-ion batteries which is also concluded by Ribiere et al. [21].

Recovery yields have not been calculated in this work as the uncertainties were too high given the difficulties in getting a stable spray and the clogging of the needles. Yields of HF of 60 to 95% were recently reported from tests in the Tewarson apparatus by Eshetu et al. [20].

In the calibration work the hydrolysis of POF_3 was not investigated. This could be an interesting issue to investigate in future studies. No special precautions were taken in order to remove traces of water in the calibration bags for POF_3 as for PF_5 and the POF_3 concentration was decreasing over time at 170°C in the cell as seen in Figure 3. This can be caused by humidity and/or temperature. This also implies that any concentration measured in the tests will depend on humidity and temperature in the exhaust gases together with local humidity, residence time and flame temperature in the fire as for all chemical species produced in a fire. The purpose of this work was, however, not to quantify in yields how much POF_3 and HF is produced depending on local conditions in the flame but to give a method of comparing different electrolytes and battery cells in fire situations in a small scale apparatus well established in the fire community. The measuring method can also be used in larger scale fire test apparatuses equipped with an exhaust gas duct to sample from, however, potential losses and response times have to be investigated.

Acknowledgment

The authors gratefully acknowledge the Swedish Fire Research Board (Grant number BF - 402-11) and the Swedish Energy Agency for the financial support.

References

1. Lisbona D, Snee T. A review of hazards associated with primary lithium and lithium-ion batteries, *Process safety and environmental protection* 2011; **89:** 434-442.
2. Larsson, F., Mellander, B-E, Abuse by external heating, overcharge and short circuiting of commercial lithium-ion battery cells, *Journal of the Electrochemical Society*, 2014; **161 (10):** A1611-A1617
3. Doughty D, Roth P, A general discussion of Li ion battery safety. *The Electrochemical Society Interface*, 2012: 37-44.
4. Campion CL, Li W, Lucht B. Thermal decomposition of LiPF6-based electrolytes in lithium-ion batteries. *Journal of the Electrochemical Society* 2005; **152 (12)**: A2327-A2334.
5. Yang H, Shen XD. Dynamic TGA-FTIR studies on the thermal stability of lithium/graphite with electrolyte in lithium-ion cell. *Journal of Power Sources* 2007;167: 515-519.
6. Lux SF, Lucas IT, Pollak E, Passerini S, Winter M, Kostecki R. The mechanism of HF formation in LiPF6 based organic carbonate electrolyte. *Electrochemistry Communications* 2012; **4**: 47-50.
7. Yang, H., Zhuang, G. V. and Ross, P. N. Jr, "Thermal Stability of $LiPF_6$ salt and Li-ion battery electrolytes containing $LiPF_6$, Journal of Power sources 161 (2006) 573-579.
8. Wang QS, Sun JH, Chu GQ, Yao XL, Chen CH. Effect of LiPF6 on the thermal behaviors of four organic solvents for lithium ion batteries. *Journal of Thermal Analysis and Calorimetry*, 2007; **89: 1**: 245-250.
9. Teng XG, Li FQ, Ma PH, Ren QD, Li SY. Study on thermal decomposition of lithium hexafluorophosphate by TG–FT-IR coupling method. *Thermochimica Acta*, 2005; **436:** 30-34.
10. Kirk-Othmer *Encyclopedia of Chemical Technology*, John Wiley & Sons, 1994, **11**.

11. Hammami A, Raymond N, Armand M. Runaway risk of forming toxic compounds, *Nature* 2003; **424**, 635-636.
12. Hygiensiska gränsvärden AFS 2011:18, Hygieniska gränsvärden Arbetsmiljöverkets föreskrifter och allmänna råd om hygieniska gränsvärden, ISBN 978-91-7930-559-8, ISSN 1650-3163, Swedish Work Environment Authority, Sweden, 2011.
13. Ohsaki T, Kishi T, Kuboki T, Takami N, Shimura N, Sato Y, Sekino M, Satoh A. Overcharge reaction of lithium-ion batteries, *Journal of Power Source* 2005; **146:** 97-100.
14. Abraham DP, Roth P, Kostecki E, McCarthy K, MacLaren S, Doughty D, Diagnostic examination of thermally abused high-power lithium-ion cells, *Journal of Power Sources* 2006;**161**: 648-657.
15. Roth P. Thermal response and flammability of Li-ion cells for HEV and PHEV applications, *SAE Int. J. Passen. Cars – Mech. Syst*, 2008, volume 1, issue 1.
16. Kawamura T., Okada, S., Yamakai, J., Decomposition reaction of LiPF6-based electrolytes for lithium ion cells, *Journal of Power Sources* 2006; **156**:547-554
17 Lekgoathi, M., D., S., Vilakazi, B., M., Le Roux, J.P., Moolman, D., Decompostion kinetics of anhydrous and moisture exposed LiPF6 salts by thermogravimetry, *Journal of Flourine Chemistry*, 2013; **149**: 53-56
18. Gachot, G., Grugeon, S., Armand, M., Pilard, S., Guenot, P., Tarascon, J-M., Laruelle, S., Deciphering the multi-step degradation meechanisms of carbonate-based electrolyte in Li batteries, Journal of Power Sources 2008; 178: 409-421
19. Eshetu,G.G., Grugeon, S., Laruelle, S., Boyanov, S., Lecocq, A., Bertrand, J-P., Marlair, G., In-depth safety-focused analysis of solvents used in electrolytes for large scale lithium ion batteries, *Phys.Chem. Chem. Phys*., 2013; **15**: 9145
20. Eshetu, G., Bertrand, J-P., Lecocq, A., Grugeon, S., Laruelle, S., Armand, M., Marlair, G., Fire behavior of cabonates-based electrolytes used in Li-ion recheragabel batteries with a focus on the role of the $LiPF_6$ and LiFSI salts, *Journal of Power Sources*, 2014; **269**,: 804-811
21. Ribière, P., Grugeon, S., Morcrette, M., Boyanov, S., Laruelle, S., Marlair G., Energy Environ. Sci., 5 (2012) 5271-5280.
22. ISO 5660:2002 Reaction-to-fire-tests – Heat release, smoke production and mass loss rate – Part 1: Heat release rate (cone calorimeter method)
23. Andersson, P., Blomqvist, P., Lorén, A., Larsson, R., Investigation of fire emissions from Li-ion batteries, SP Report 2013:5, SP Technical Research Institute of Sweden, Boras, Sweden, ISBN 978-91-87461-00-2, 2013.
24. ISO 19702:2006, Toxicity testing of fire effluents -- Guidance for analysis of gases and vapours in fire effluents using FTIR gas analysis
25. Larsson. F., Andersson, P., Blomqvist,P., Lorén, A., Mellander, B-E, Characteristics of Lithium-ion batteries during fire tests, *Journal of Power Sources*, 2014**; 271**,: 414-420.
26. EN 13823:2010, Reaction to fire tests for building products – Building products excluding floorings exposed to the thermal attack by a single burning item
27. Fu, Y., Lu, S., Li, K., Liu, C., Cheng, X., Zhang, H., An experimental study on burning behaviors of 18650 lithium ion batteries using cone calorimeter, *Journal of Power Sources* 2015; **273**: 216-222
28. Gachot, G, Grugeon, S., Jimenez-Gordon, I., Eshetu, G., Boyanov, S:, Lecocq, A:, Marlair, G., Pilard, S., Gas chromatography/Fourier transform infrared/mass spectrometry coupling: a tool for Li-ion battery safety field investigation, Anal. Methods, 2014, **6**, 6120-6124

Table 1 Specification of the FTIR measurement system.

Instrumentation*	**Specification**
Primary filter	M&C** PSP 4000M (filtration chamber volume 40 cm^3) with ceramic filter (SP-2K, length 75 mm) heated to 180 °C
Sampling tubing	4/6 mm diameter PTFE tubing heated to 180°C. The length of the tubing was 2.5 m (before secondary filter) + 1.5 m (after secondary filter)
Secondary filter	M&C** FSS-3SS/H350 (filtration chamber volume 130 cm^3) with sintered steel filter (type SS316, length 150 mm) heated to 180°C
Gas cell	Volume: 0.2 litres Path length: 2.0 m Temperature: 180°C Cell pressure: 650 Torr
Pump	Sampling flow: 3.5 l/min
Spectrometer	Thermo Scientific Antaris IGS analyzer (Nicolet)
Spectrometer parameters	Resolution: 0.5 cm-1 Spectral range: 4800 cm^{-1} – 650 cm^{-1} Scans/spectrum: 10 Time/spectrum: 12 seconds Detector: MCT

* Components of the sampling system presented in order occurring in the sampling stream.
** M&C TechGroup Germany GmbH

Table 2 Spectral band positions for POF_3.

Band position (cm^{-1})	Absorptivity* (abs/ppm.m)	Type of band [13]
1416	0.0014	P-O stretch
991	0.0014	P-F asymmetrical stretch
871	0.00025	P-F symmetrical stretch

* Calculated from a spectrum of 100 ppm POF_3 (650 Torr, 180 °C).

Table 3 Spectral band positions found from PF_5 and decomposition products.

Band position (cm^{-1})	**Type of band**
1017	PF_5: PF stretching [13]
946	PF_5: PF stretching [13]
1027	Band from unknown decomposition product
956	Band from unknown decomposition product
1416	POF_3: P-O stretch
991	POF_3: P-F asymmetric stretch
871	POF_3: P-F symmetric stretch

Table 4. Test conditions and results in the burner tests

Test	Type of distribution method for electrolyte	Flow of electrolyte (ml/min)	Salt in electrolyte	Burner (propane) HRR	HRR from combustion of electrolyte	HF/POF_3 ratio
A	Needle	18	0.4 M in DME	4 kW	6 kW	53
B	Needle	18	1 M in DMC	4 kW	4 kW	14
C	Needle	18	1 M in DMC	4 kW	4 kW	20
D	Metal plate	1.8	1 M in DMC	4 kW		8
E	Needle	15	1 M in DMC	5 kW	3 kW	23
F	Needle	15	0.4 M in DMC	3.2 kW	2.5 kW	20
G	Needle	15	1 M in DMC	5 kW	3.3 kW	12
H	Needle, water spray	15	1 M in DMC	5 kW	3 kW	8
I	Needle, water spray	15	1 M in DMC	5 kW	2 kW	16